



MIT Open Access Articles

Trypsin Pre#Treatment Combined With Growth Factor Functionalized Self#Assembling Peptide Hydrogel Improves Cartilage Repair in Rabbit Model

The MIT Faculty has made this article openly available. **Please share** how this access benefits you. Your story matters.

As Published	10.1002/JOR.24414
Publisher	Wiley
Version	Author's final manuscript
Citable link	https://hdl.handle.net/1721.1/136393
Terms of Use	Creative Commons Attribution-Noncommercial-Share Alike
Detailed Terms	http://creativecommons.org/licenses/by-nc-sa/4.0/



Published in final edited form as:

J Orthop Res. 2019 November ; 37(11): 2307–2315. doi:10.1002/jor.24414.

Trypsin Pre-Treatment Combined with Growth-Factor Functionalized Self-Assembling Peptide Hydrogel Improves Cartilage Repair in Rabbit Model

Gustavo Zanotto¹, Paul Liebesny², Myra Barrett¹, Hannah Zlotnick², Alan Grodzinsky², David Frisbie^{1,*}

¹Orthopaedic Research Center, Department of Clinical Sciences, College of Veterinary Medicine and Biomedical Sciences, Colorado State University, 300 West Drake Road, Fort Collins, CO 80523.

²Center for Biomedical Engineering, Department of Biological Engineering, Massachusetts Institute of Technology, 500 Technology Square, Cambridge, MA 02139.

Abstract

The objective of this study was to improve cartilage repair and integration using self-assembling KLD hydrogel functionalized with platelet derived growth factor-BB and heparin-binding insulin like growth factor-1 with associated enzymatic trypsin pre-treatment of the native cartilage. Bilateral osteochondral defects were created at the central portion of the femoral trochlear groove of 48 skeletally mature, white New Zealand rabbits. One limb received a randomly assigned treatment and the contralateral limb served as the control. Treated defects were exposed to trypsin for 2 minutes and filled with self-assembling KLD hydrogel only, or associated to growth factors. All control limbs received KLD hydrogel alone or received only trypsin but not hydrogel. Ninety days post-defect creation, the rabbits were euthanized and magnetic resonance imaging, radiography, macroscopic evaluation, histology and immunohistochemistry of the joint and repaired tissue were performed. Mixed model analyses of variance were utilized to assess the outcome parameters and individual comparisons were performed using Least Square Means procedure and differences with p -value <0.05 were considered significant. Trypsin enzymatic pre-treatment improved cellular morphology, cluster formation and subchondral bone reconstitution. Platelet derived growth factor-BB growth factor improved subchondral bone healing and basal integration. Heparin-binding insulin like growth factor-1 associated with platelet derived growth factor improved tissue and cell morphology. The authors conclude that self-assembling KLD hydrogel functionalized with platelet derived growth factor and heparin-binding insulin like growth factor-1 with associated enzymatic pre-treatment of the native cartilage with trypsin resulted in an improvement on the cartilage repair process.

*Corresponding author: David Frisbie, Translational Medicine Institute, Colorado State University, 2350 Gillette Drive, Fort Collins, CO 80523 (current address), david.frisbie@colostate.edu, Ph (970) 297-4555, Fax (970) 297-4138.

Author Contribution Statement

All authors contributed to conception and design, acquisition, analysis and interpretation of the data, critical review of the article and read and approved the final submitted manuscript.

All the other authors declare no conflict of interest.

Keywords

cartilage repair; self-assembling peptide hydrogel; trypsin; growth factors

Clinicians are still seeking a technique that returns damaged cartilage to its original state, although many consider subchondral bone microfracture the standard of care. However, after microfracture, the repaired tissue is composed of fibrous cartilage^{1, 2} coupled with poor horizontal integration, which may account for the higher re-operation rate long-term (10 years) when compared to more involved or aggressive procedures of cartilage repair such as osteochondral autograft/allograft and second-generation autologous chondrocyte transplantation.³ While these advanced techniques have an improved long-term outcome, they are not without significant challenges. In this study, we explored ways to improve the repair tissue characteristics as well as the horizontal integration following microfracture.

Self-assembling peptide hydrogel scaffold has shown promise in augmenting microfracture.⁴ The self-assembling capacity allows this product to be injected arthroscopically, and its high water content allows cells to migrate and deposit extracellular matrix. Self-assembling KLD hydrogel has proven to be biocompatible and stimulate cartilage repair by improving defect filling and increasing in tissue properties.⁵ It can also act as a carrier of other molecules if desired. Safety, feasibility and clinical improvement in cartilage healing have previously been observed with self-assembling KLD hydrogel using critically sized chondral defects in a long-term equine model with strenuous exercise.⁶

It has been demonstrated that the chondrocytes present in the native cartilage have a limited capacity to proliferate and migrate. For that reason, undifferentiated mesenchymal stem cells (MSCs) present in the marrow cavity are often targeted as a cell population to augment cartilage damage.⁷ Several growth factors have been studied to stimulate MSC proliferation and migration into the defect.⁸ Recently, platelet-derived growth factor (PDGF) and transforming growth factor B1 (TGF-B1) have been shown to increase MSC migration into the self-assembling KLD hydrogel. In this same study, heparin-binding insulin like growth factor 1 (HB-IGF-1) stimulated extracellular matrix (ECM) deposition within the scaffold and in surrounding cartilage.⁴ We sought to assess the improved healing with these growth factors through delivery with self-assembling KLD hydrogel.

The lack of the neo synthesized cartilage integration with the surrounding cartilage is believed, by some, to result in instability of the repair tissue, leading to tissue degeneration.⁷ The lack of cartilage-to-cartilage or horizontal integration is not completely understood; however, several factors seem to play an important role, including low chondrocyte viability in the surrounding cartilage, and dense surrounding ECM.⁹ Horizontal integration could be improved by utilizing chemotactic agents to attract more viable chondrocytes to this area, or by enzymatic digestion of the surrounding cartilage. Horizontal integration has been shown to be highly dependent on collagen deposition and cross-linking^{10, 11} as well as cellular repopulation.¹² Several proteolytic enzymes have been studied to improve cartilage integration.¹³ Recently the authors' demonstrated that enzymatic pretreatment of cartilage explants with trypsin for 2 minutes was able to promote proteoglycan depletion on the surrounding cartilage up to 200 μm , which resulted in increased cellular migration to this

region.¹⁴ This enzymatic pretreatment was then followed by a fetal bovine serum (FBS) rinse to neutralize and remaining trypsin.

The present study evaluated cartilage repair and integration using self-assembling KLD hydrogel functionalized with PDGF and HB-IGF-1 associated enzymatic pre-treatment of the native cartilage using trypsin in a rabbit model. We hypothesize that self-assembling KLD hydrogel functionalized with PDGF and HB-IGF-1 associated enzymatic trypsin pre-treatment will result in improved cartilage repair and horizontal (cartilage-to-cartilage) integration with the surrounding native tissue.

METHODS

Study design

The Institutional Animal Care and Use Committees of Colorado State University, protocol # 15-5769A, approved all aspects of this study. White, female, New Zealand rabbits (Western Oregon Rabbit Company, USA) were used in the present study (N=48). Forty-four skeletally mature/aged (14 months) rabbit were used in this study, and to compare the effect of rabbit age, four 7-month-old rabbits were also utilized but not included in the statistical analysis. Bilateral critically sized defects were created (3 mm diameter x 2 mm deep) in the central portion of the trochlear groove using a drill bit and customized guide. One leg was randomly selected to receive the treatment and the contralateral served as a control. Details about animal management, anesthesia protocol and surgery can be found in supplemental material (Table S-4 and S-5, and Figure S-1).

Treatments

The study occurred in two temporal blocks due to the number of animals used. All trypsin-treated defects were followed with subsequent inactivation with FBS for 2 minutes. In total, five treatment combinations and 2 different controls were used (Table 1): 1) KLD+Trypsin group (24 limbs): Defect exposed to trypsin for 2 minutes, followed by filling the defect with KLD hydrogel; 2) KLD+HB-IGF-1 group (8 limbs): Defect filled with KLD premixed with 615nM HB-IGF-1 before assembly; 3) KLD+Trypsin+HB-IGF-1 group (8 limbs): Trypsin treatment, followed by filling the defect with KLD premixed with 615nM HB-IGF-1; 4) KLD+Trypsin+PDGF group (12 limbs): Trypsin treatment, followed by filling the defect with 100ng/ml of PDGF-BB premixed in KLD and 5) KLD+Trypsin+HB-IGF-1+PDGF group (12 limbs): Trypsin treatment, followed by filling the defect with 100ng/ml of PDGF-BB plus 615nM of HB-IGF-1 premixed in KLD. Control defects were treated with KLD only (24 limbs), which consisted of filling the defect with KLD hydrogel, gently flushing with saline solution and allowing 5 minutes for hydrogel assembly, or defects were left empty (8 limbs), or defects received the trypsin treatment and no hydrogel.

Post-operative/ Endpoint procedures

Three months after surgery, all animals were euthanized (Table S-4). The circumferential measurement of each leg at one centimeter proximal to the patella was recorded as a measure of muscle mass. Joints were placed in 50 mL conical tube and kept at 4 C° for MRI analyses.

Magnetic Resonance Imaging

Images were acquired using a 2.4 Tesla nuclear magnetic resonance machine (Bruker Biospec Avance /30 cm). The imaging protocol consisted of transverse and sagittal fat-saturated proton density (PDFS) and spoiled gradient echo (SPGR) sequences; both with 1mm slice thickness and $256 \times 256 \mu\text{m}$ in plane resolution. A board-certified radiologist read the images and classified subchondral bone reconstitution in a 0 to 100% grading scale, where 0 was no subchondral bone reconstitution and 100% was complete subchondral bone reconstitution (at the level of the surrounding tissue). Defect filling was scored using a 0 to 4 grading scale with 0= 100%, 1= 99 – 75%, 2= 74–50%, 3=49–25% and 4= 24–0% of defect filled. Surface regularity, subchondral bone sclerosis and integrity were scored using a 0 to 4 ordinal grading scale with 0 = normal, 1= slight, 2 = mild, 3 = moderate and 4 being severely abnormal.

Radiography

The femorotibial joint was radiographed acquiring cranio-caudal and latero-medial images, which were scored for osteophyte formation, defect visualization and sclerosis around the defect using a 0 to 4 ordinal grading scale with 0 = normal, 1= slight, 2 = mild, 3 = moderate and 4 being severely abnormal.

Gross Pathologic Evaluation of the Joint

Gross evaluation of the repaired tissue was performed by two blinded evaluators using both previously reported¹⁵ and ICRS criteria. Joint appearance was classified as a global score including inflammation of the synovial membrane and presence of osteophytes.

Histology and Immunohistochemistry

After the macroscopic evaluation, synovial membrane was harvested and fixed for 48 hours in 10% formol. A 1.5cm long by 1cm wide and 1cm deep block including the defect and surrounding normal tissue was harvested from the distal femur with an Exakt bandsaw and fixed for 72 hours in 10% formol 1% zinc solution (Z-fix, Anathec Ltd., Battle Creek, MI), followed by decalcification with 10% formic acid (Immunocal, Statlab, McKinney, TX) for 5 days at room temperature. After complete decalcification, the samples were placed in PBS solution at 4°C until processed.

The osteochondral defect was equally divided transversely and the distal portions dehydrated and paraffin embedded for routine histology/immunohistochemistry, while the proximal portion was embedded in optimal cutting temperature compound (TissueTek OCT Sakura Finetek USA, Torrance, CA) for immunohistochemistry.

For routine histology, 5 μm thick sections were created from paraffin embedded blocks of each sample and transferred to slides followed by staining with hematoxylin/eosin and safranin–O/fast green. Two blinded evaluators scored each section using ICRSII¹⁶ microscopic score system for cartilage repair. Synovial membrane samples were evaluated for cellular infiltration, vascularity, intimal hyperplasia, subintimal edema and fibrosis using a previously described 0–4 score system (0= normal, 1, slight, 2= mild, 3 = moderate, 4 severe).⁶

Immunohistochemistry for collagen type II and aggrecan was performed using paraffin embedded samples, while frozen samples embedded in OCT were used for pro-collagen type I immunostaining. Paraffin blocks were cut in 5 μm thick sections and mounted on regular histology slides. An antigen retrieval step was performed with protein kinase (37°C for 17 minutes) for collagen type II and protein kinase (37°C for 15 minutes) plus chondroitinase ABC (37°C for 30 minutes) (Sigma-Aldrich, Saint Louis, MO) for aggrecan immunostaining. After the antigen retrieval step, sections were incubated with primary antibody solution for collagen type II at neat concentration (Collagen II #II-II6B3, Hybridoma Bank) or aggrecan at 1:100 (Alexis Biochemicals, San Diego, CA). Pro-collagen type I immunostaining was performed using 8 μm thick sections created from frozen samples embedded in OCT. The tissues were transferred and mounted on slides using CryoJane Tape-Transfer System (Leica Biosystems, Buffalo Grove, IL). Slides were incubated in acetone for 10 minutes at -20°C for tissue fixation. Sections were incubated in mouse anti pro-collagen type I antibody at neat concentration (Hybridoma Bank Cat#M-38). For all immunostaining, the endogenous peroxidase was blocked using 0.3% H_2O_2 in methanol. Sections were incubated with goat anti-mouse HRP secondary antibody solution at 1:500 (collagen type II and procollagen type I) or 1:250 (aggrecan) (Jackson Immunoresearch, Westgrove, PA) and stained with Vector Nova RED (Vector Laboratories, Burlingame, CA). Control sections were incubated with protein matched negative control solution and gave no signal. Non-calcified tissues were evaluated blindly by two evaluators for the percentage of repair tissue stained positive (0=no stain, 1=1–25%, 2=26–50%, 3=51–75%, 4=76–100%).

Statistical Analyses

Data analyses were performed using SAS version 9.4 (Cary, NC). The effect of *Trypsin* was analyzed as a main effect independently or averaging over all other effects. The effect of Growth Factor (HB-IGF1 and/or PDGF-BB) was analyzed as a main effect as well as their interaction in animals that had KLD and Trypsin in the contralateral limb. The main effect of KLD hydrogel was analyzed for animals that had trypsin as contralateral limbs. For the three previously described analyses (Trypsin, Growth Factor and KLD hydrogel) the model included subject as a random effect. Further, when a main or interaction effect had p-value < 0.05, individual comparisons were performed using Least Square Means (LSMeans) procedure and differences with p-value < 0.05 were considered significant. LSMeans and 95% confidence limits are reported.

RESULTS

Magnetic Resonance Imaging

Trypsin pre-treatment was associated with improved (13%) subchondral bone reconstitution (trypsin= 46.11 (38.70 – 53.52, LSMeans (95% CI)) and control= 33.20 (22.76 – 43.65); p=0.047) (Figure 1). MRI defect filling was on average between 50 to 75% category with trypsin resulting in slightly more defect filling compared to controls (trypsin= 1.9 (1.6 – 2.1) and control= 2.5 (2.1 – 2.9); p=0.008). Overall, reparative tissue had a mildly irregular surface with trypsin treated defects having slightly smoother surface than control (trypsin=

2.0 (1.7 – 2.2) and control= 2.5 (2.1 – 2.9); $p=0.014$). No significant growth factor main effect or interactions were observed (Table S-1).

Radiography

Trypsin pre-treatment did not result in statistically significant differences for any parameters evaluated by radiography. However, PDGF-BB mildly increased subchondral bone healing, defined as decreased defect visualization on radiography (PDGF-BB= 1.43 (1.01 – 1.84) and control= 2.05 (1.64 – 2.45); $p= 0.0170$). Osteophytes were not radiographically observed in defects treated with self-assembling KLD hydrogel, however some were present on control defects (KLD hydrogel= 0.08 (–0.13 – 0.30) and control= 0.71 (0.32 – 1.10); $p=0.008$) (Table S-1).

Gross Pathologic Evaluation of the Joint

Pre-treatment with trypsin demonstrated a slight but significant reduction in muscle atrophy (based on the circumferential measurement of each leg at one centimeter proximal to the patella) (trypsin= 13.33 (13.20 – 13.47) and control= 13.17 (13.03 – 13.31); $p< 0.05$), mild improvement of cartilage firmness (trypsin= 0.86 (0.68 – 1.03) and control= 1.17 (0.93 – 1.41); $p= 0.0322$) and a shift from yellow/white to white repair tissue color (trypsin= 5.20 (5.08 – 5.32) and control= 5.84 (5.66 – 6.01); $p= 0.0001$), as well as slightly improvement on total cumulative macroscopic score (trypsin= 17.32 (16.42 – 18.21) and control= 18.79 (17.59 – 19.99); $p= 0.0391$). Even though the defects treated with trypsin resulted in slightly higher values of joint inflammation (trypsin= 0.41 (0.24 – 0.58) and control= 0.07 (–0.13 – 0.28); $p= 0.0027$) and synovial membrane proliferation (trypsin= 0.86 (0.64 – 1.07) and control= 0.48 (0.19 – 0.77); $p= 0.032$), these values were still under the “slightly affected” category. PDGF-BB treated joints showed slightly more joint inflammation compared to joints that did not received PDGF-BB (PDGF-BB= 0.60 (0.32 – 0.87) and control= 0.24 (–0.02 – 0.51); $p=0.0314$). Joints which had the defects filled with self-assembling KLD hydrogel were closer to normal in appearance while defects not filled with KLD evidenced slight inflammation (KLD hydrogel= 0.16 (–0.08 – 0.42) and control= 1.0 (0.55 – 1.44); $p=0.002$) (Table S-2). Qualitatively, young animals demonstrated improved cartilage integration compared to older), however formal statistical analyses were not performed due to low numbers of animals included.

Histology

Synovial membrane—There is a main effect for trypsin enzymatic pre-treatment in reducing the grade of the synovial membrane intimal hyperplasia by about half (Trypsin = 0.55 (0.31 – 0.78) and control = 0.96 (0.62 – 1.30); $p= 0.05$). All the other parameters were not statistically significantly different (Table S-3).

Osteochondral histology—Trypsin pre-treatment improved cell morphology in 20% (trypsin= 79.83 (73.48 – 86.17) and control= 59.83 (50.86 – 68.8); $p= 0.0005$) (Figure 2) and slightly decreased (less than 10%) the number of cell clusters observed (trypsin= 88.41 (85.04 – 91.78) and control= 82.00 (77.23 – 86.76); $p= 0.0317$). A trend ($p=0.059$) for trypsin treatment to improve tissue morphology was also observed, (trypsin= 51.49 (45.38 – 57.61) and control= 41.47 (32.90 – 50.05)). However, trypsin pre-treatment slightly increased

(less than 10%) repaired tissue vascularization (trypsin= 92.08 (87.74 – 96.42) and control= 99.58 (93.67 – 105.5); p= 0.035).

PDGF-BB resulted in 23% improvement on chondrocyte cell morphology (PDGF-BB= 88.62 (76.97 – 100.28) and control= 65.21 (55.13 – 75.29); p= 0.0037) and 16% increase in basal integration of the repair tissue with the underlying bone (Figure 3) compared to defects not treated with PDGF-BB (PDGF-BB= 86.12 (75.39 – 96.85) and control= 70.69 (61.40 – 79.97); p=0.0337).

The addition of PDGF-BB and HB-IGF-1 resulted in a significant effect over HB-IGF-1 alone (p=0.0100). Specifically, with respect to improvement in tissue morphology (HB-IGF-1 + PDGF-BB= 66.25 (50.07 – 82.42) and HB-IGF-1= 36.25 (20.07 – 52.42); p=0.01) as well as chondrocyte morphology (Figure 4 and 5): (HB-IGF-1 + PDGF-BB= 96.25 (78.88 – 113.62) and HB-IGF-1= 50.00 (32.63 – 67.36); p=0.0046). Also, the combination of HB-IGF-1 and PDGF-BB resulted in about 20% less subchondral bone abnormalities/marrow fibrosis compared to HB-IGF-1 alone (HB-IGF-1 + PDGF-BB= 92.23 (80.75 – 103.71) and HB-IGF-1= 72.50 (61.01 – 83.98); p= 0.0174).

Chondrocyte clustering was observed to be significantly greater when the defects were treated with HB-IGF-1 or PDGF-BB alone compared to control defects. When these growth factors were combined there was no statistical difference when compared to controls (control= 91.14 (85.74 – 96.54), HB-IGF-1= 80.00 (70.89 – 89.10), PDGF-BB= 80.90 (72.52 – 89.27) and HB-IGF1 + PDGF-BB= 88.01 (78.60 – 97.42); p= 0.032) (Table S-3).

Even though formal statistical analysis was not performed comparing animals by age, young animals demonstrated on average, more reparative tissue matrix metachromasia and decreased vascularization.

Immunohistochemistry—There is a main effect of trypsin or PDGF-BB to induce more pro-collagen type I immunostaining compared to control (trypsin= 2.19 (1.83 – 2.55) and control= 1.43 (0.92 – 1.95); p= 0.0187) (PDGF-BB= 2.56 (1.92 – 3.20) and control= 1.71 (1.12 – 2.30); p=0.055) (Figure 6). Defects treated with self-assembling KLD hydrogel had significantly more aggrecan than those left empty (KLD hydrogel= 3.72 (3.40 – 4.04) and controls= 2.87 (2.34 – 3.40); p= 0.0092). Aggrecan and collagen type II immunostaining did not demonstrate any statistically significant differences based on presence of growth factors (Table S-3).

DISCUSSION

Some of the reasons for cartilage repair failure are related to the poor quality of the neo-synthesized tissue, which usually consists of more fibrocartilage than hyaline cartilage, and the poor integration of the neo cartilage to the surrounding tissue.⁷ In the present study, trypsin pre-treatment of the osteochondral defect resulted in slight improvement of the defect filling, subchondral bone reconstitution and surface regularity observed on MRI, as well as slight improvement cartilage firmness and color on gross appearance; and mild improvement in cell morphology and cluster formation histologically. Considering all of these findings together, along with the reduced muscle atrophy observed with trypsin treated

defects, the authors' believe trypsin pre-treatment induced an overall modest improvement in cartilage repair which led to better use (evidence by decreased muscle atrophy) of the treated limb compared to the contralateral limb.

Recently our group demonstrated that enzymatic pre-treatment of cartilage explants with trypsin for 2 minutes were able to promote proteoglycan depletion extending from the center of the cartilage annuli in about 200 μm thick, dramatically influencing cellular migration and promoting better cartilage horizontal integration in an *in vitro* model.¹⁴ Trypsin enzymatic pre-treatment of the cartilage results in proteoglycan depletion in a time dependent manner, not affecting collagen network¹⁷ and results in increased cell volume and total proteoglycan deposition on partial thickness cartilage defects in rabbits.¹⁸ Furthermore, chondrocyte proliferation was shown to increase post intra-articular injection of trypsin in rabbits.¹⁹

The trypsin pretreatment mildly increased synovial membrane proliferation and slightly increased macroscopic joint inflammation (scale: normal, slight, mild, moderate or severe categories). These findings were in contrast to previous reports where trypsin was injected intra-articularly at a much higher concentration (100x more concentrated than in this study).¹⁸⁻²⁰ In these reports, trypsin did not result irritation of the synovial membrane macroscopically. In the present study, our macroscopic results differ from our histologic findings where trypsin resulted in less histologic synovial membrane intimal hyperplasia, suggesting lack of active inflammation. Without histologic abnormalities the level of macroscopic change most likely is not of clinical significance.

In the current study, the combination of HB-IGF-1 and PDGF-BB seems to mitigate the negative impact of HB-IGF-1 on cell and tissue morphology. The authors chose this combination of growth factors because PDGF and IGF-1 have been reported to be the most potent agents capable of induction of bone marrow-MSc migration when 16 chemokines were assessed.²¹ Similarly, in an *in vitro* rabbit model this combination also showed superior chemotactic effects on MSC's compared to either growth factor alone.²² The authors believe this is the first example of an *in vivo* application of these growth factors in a cartilage repair model, which supports our *in vitro* work.⁴

In the current study PDGF-BB alone was noted to have a significant effect improving radiographic subchondral bone healing (30%) and histologic basal integration (16%) of the repair tissue when compared to controls. PDGF has been shown to induce bone repair²³, but also inhibit endochondral differentiation.²⁴ Subchondral bone reconstitution is mainly derived by two different mechanism of bone production: endochondral and direct intramembranous ossification.⁷ Thus, given PDGF's capacity to improve intramembranous ossification and our observed improved subchondral bone healing and increased basal integration the authors credit these observations to PDGF.

Ultimately, we would expect reformation of the tidemark with improved bone healing, which was not observed in the current study. However, the current study period of 12 weeks was most likely too short to have expected significant tidemark reformation as this has been reported to take 24 weeks⁷ in other work. A longer-term study would be needed to better address this effect.

In the current study, a significant increase in osteophyte formation was observed with PDGF-BB treatment when compared to control, but its noteworthy this difference was slightly and may be of questionable clinical significance. Such findings of increased osteogenic activity on the subchondral bone have been previously reported.²⁵ In this way, it is possible that the slight increase in osteophyte formation may be related to a higher subchondral bone activity, since no other signals of active inflammation or instability were noticed in the current study outcome parameters (radiographic and histologic).

Surprisingly, no significant main effects of HB-IGF-1 on proteoglycan deposition were observed. Insulin Growth Factor-1 has been studied in cartilage repair and has been reported both in vitro and in vivo to significantly improve chondrogenesis and cartilage integration.^{26–29} Our group has reported that HB-IGF-1 is strongly retained in articular cartilage post intra-articular injection³⁰ and leads to sustained proteoglycan biosynthesis in cartilage explants.³¹ Interestingly, an in vitro kinetics study showed that 84% of the HB-IGF-1 that was premixed into a KLD hydrogel was released within the first four days of culture⁴; however, this HB-IGF-1 seems to be bound by surrounding cartilage annuli instead of being released in the media¹⁴. Further studies are necessary to elucidate the lack of effect in the present study.

When assessing the effect of KLD hydrogel we observed a 32% increase (3.7 vs 2.8) in aggrecan deposition and a 90% improvement (0.1 vs 1) in macroscopic joint observation when compared to defects not treated with KLD hydrogel. These findings are consistent with our previous studies.^{5, 6}

We used MRI, as it can be potentially used as a non-invasive imaging modality in future studies, to quantitatively describe the healing process in hopes that this technique may be used in future human patients. MRI outcomes demonstrate a 39% improvement of subchondral bone healing with trypsin treatment compared to control (46 vs 33, respectively). Similarly, we also observed a 24% improvement (1.9 vs 2.5) in defect filling and 20% improvement (2.0 vs 2.5) in surface regularity with trypsin treatment in a similar comparison. These results suggest an improvement with trypsin treatment as well as usefulness of the MRI outcomes.

The authors have been utilizing older rabbits, at least 12 months old, to assess cartilage healing techniques as we believed that younger rabbits have a greater propensity to heal and maybe provide overly optimistic outcomes. In the current work we included four (N=4) 7-month-old rabbits. Due to the low numbers statistical analyses were not attempted but rather qualitative data assessed. Young adult (7-month-old) rabbits tended to have improved scores when compared to the older rabbits. Some of the most striking improvements were in cartilage integration (macroscopically), and histologic matrix metachromasia as well as vascularization. Previous reports support our subjective findings that seven to eight-month-old New Zealand white rabbits have a decreased healing of full thickness cartilage defect, compared to 5 (adolescent) and 3 (immature) month-old.³² The authors are unaware of other publications comparing 7 (skeletally mature) to 14-month-old (aged) rabbits as done in the current study.

The authors utilized the current rabbit model to help ascertain the best treatment group(s) to assess in a large (equine) animal model. It was accepted that using the rabbit as a test species included inherent limitations as highlighted by a robust intrinsic healing capacity (90% of the defect area and 80% of defect volume were reconstituted across all treatment/control groups). Despite limitations in the current study, it did offer insight to treatments resulting in significant improvements to guide further studies.

CONCLUSION

Trypsin enzymatic pretreatment of the surrounding cartilage resulted in modest positive effects of several parameters evaluated in this study (muscle atrophy, defect filling, subchondral bone reconstitution, surface regularity, cartilage firmness and color, cell morphology and cluster formation). The combination of both growth factors seems to have more beneficial effects than when each growth factor is used alone. Further studies in a long-term, large animal model are warranted to further investigate the potential clinical benefits of these findings.

Supplementary Material

Refer to Web version on PubMed Central for supplementary material.

ACKNOWLEDGMENT

We thank Dr. Richard Lee (Brigham & Women's Hospital, Boston, MA) for kindly providing HB-IGF-1 and 3-D Matrix (Waltham, MA) for donating KLD hydrogel. We also thank Christine Battaglia and Melinda Meyers from all the laboratory support and Elisa French for animal care. This project was funded by NIH-NIAMS Grant AR060331 and Brazilian National Council of Scientific and Technologic Development -CNPq (pre-doctoral scholarship to GZ). Dr. Grodzinsky has equity in 3D-Matrix (Japan).

REFERENCES

1. Frisbie DD, Trotter GW, Powers BE, et al. 1999 Arthroscopic subchondral bone plate microfracture technique augments healing of large chondral defects in the radial carpal bone and medial femoral condyle of horses. *Vet Surg* 28: 242–255. [PubMed: 10424704]
2. Erggelet C, Vavken P. 2016 Microfracture for the treatment of cartilage defects in the knee joint - A golden standard? *J Clin Orthop Trauma* 7:145–152. [PubMed: 27489408]
3. Riboh JC, Cvetanovich GL, Cole BJ, Yanke AB. 2017 Comparative efficacy of cartilage repair procedures in the knee: a network meta-analysis. *Knee Surg Sports Traumatol Arthrosc* 25: 3786–3799. [PubMed: 27605128]
4. Liebesny PH, Byun S, Hung HH, et al. 2016 Growth Factor-Mediated Migration of Bone Marrow Progenitor Cells for Accelerated Scaffold Recruitment. *Tissue Eng Part A* 22: 917–927. [PubMed: 27268956]
5. Miller RE, Grodzinsky AJ, Vanderploeg EJ, et al. 2010 Effect of self-assembling peptide, chondrogenic factors, and bone marrow-derived stromal cells on osteochondral repair. *Osteoarthritis Cartilage* 18:1608–1619. [PubMed: 20851201]
6. Miller RE, Grodzinsky AJ, Barrett MF, et al. 2014 Effects of the combination of microfracture and self-assembling Peptide filling on the repair of a clinically relevant trochlear defect in an equine model. *J Bone Joint Surg Am* 96: 1601–1609. [PubMed: 25274785]
7. Shapiro F, Koide S, Glimcher MJ. 1993 Cell origin and differentiation in the repair of full-thickness defects of articular cartilage. *J Bone Joint Surg Am* 75: 532–553. [PubMed: 8478382]
8. Fortier LA, Barker JU, Strauss EJ, et al. 2011 The role of growth factors in cartilage repair. *Clin Orthop Relat Res* 469: 2706–2715. [PubMed: 21403984]

9. Khan IM, Gilbert SJ, Singhrao SK, et al. 2008 Cartilage integration: evaluation of the reasons for failure of integration during cartilage repair. A review. *Eur Cell Mater* 16: 26–39. [PubMed: 18770504]
10. DiMicco MA, Sah RL. 2001 Integrative cartilage repair: adhesive strength is correlated with collagen deposition. *J Orthop Res* 19: 1105–1112. [PubMed: 11781012]
11. DiMicco MA, Waters SN, Akeson WH, Sah RL. 2002 Integrative articular cartilage repair: dependence on developmental stage and collagen metabolism. *Osteoarthritis Cartilage* 10: 218–225. [PubMed: 11869083]
12. Bos PK, DeGroot J, Budde M, et al. 2002 Specific enzymatic treatment of bovine and human articular cartilage: implications for integrative cartilage repair. *Arthritis Rheum* 46: 976–985. [PubMed: 11953975]
13. Boushell MK, Hung CT, Hunziker EB, et al. 2017 Current strategies for integrative cartilage repair. *Connect Tissue Res* 58: 393–406. [PubMed: 27599801]
14. Zlotnick HM AA, Chen HJ, Liebesny PH, et al. 2019 Tissue Engineering. Enzyme Pretreatment Plus Locally Delivered HB-IGF-1 Stimulates Integrative Cartilage Repair In Vitro. *Tissue Engineering Part A*. In press.
15. Frisbie DD, Bowman SM, Colhoun HA, et al. 2008 Evaluation of autologous chondrocyte transplantation via a collagen membrane in equine articular defects: results at 12 and 18 months. *Osteoarthritis Cartilage* 16: 667–679. [PubMed: 18042409]
16. Mainil-Varlet P, Van Damme B, Nestic D, et al. 2010 A new histology scoring system for the assessment of the quality of human cartilage repair: ICRS II. *Am J Sports Med* 38: 880–890. [PubMed: 20203290]
17. Griffin DJ, Vicari J, Buckley MR, et al. 2014 Effects of enzymatic treatments on the depth-dependent viscoelastic shear properties of articular cartilage. *J Orthop Res*. 32: 1652–1657. [PubMed: 25196502]
18. Quinn TM, Hunziker EB. 2002 Controlled enzymatic matrix degradation for integrative cartilage repair: effects on viable cell density and proteoglycan deposition. *Tissue Eng*. 8: 799–806. [PubMed: 12459058]
19. Havdrup T 1979 Trypsin-induced mitosis in the articular cartilage of adult rabbits. *Acta Orthop Scand* 50:15–19. [PubMed: 425826]
20. Lack W, Bosch P, Lintner F. 1986 Influence of trypsin on the regeneration of hyaline articular cartilage. *Acta Orthop Scand* 57: 123–125. [PubMed: 2422868]
21. Ponte AL, Marais E, Gallay N, et al. 2007 The in vitro migration capacity of human bone marrow mesenchymal stem cells: comparison of chemokine and growth factor chemotactic activities. *Stem Cells*. 25: 1737–1745. [PubMed: 17395768]
22. Ozaki Y, Nishimura M, Sekiya K, et al. 2007 Comprehensive analysis of chemotactic factors for bone marrow mesenchymal stem cells. *Stem Cells Dev* 16: 119–129. [PubMed: 17348810]
23. Chung R, Foster BK, Zannettino AC, Xian CJ. 2009 Potential roles of growth factor PDGF-BB in the bony repair of injured growth plate. *Bone*. 44: 878–885. [PubMed: 19442606]
24. Kieswetter K, Schwartz Z, Alderete M, et al. 1997 Platelet derived growth factor stimulates chondrocyte proliferation but prevents endochondral maturation. *Endocrine* 19: 257–264.
25. Hulth A, Johnell O, Miyazono K, et al. 1996 Effect of transforming growth factor-beta and platelet-derived growth factor-BB on articular cartilage in rats. *J Orthop Res* 14: 547–553. [PubMed: 8764863]
26. Fortier LA, Mohammed HO, Lust G, Nixon AJ. 2002 Insulin-like growth factor-I enhances cell-based repair of articular cartilage. *J Bone Joint Surg Br* 84: 276–288. [PubMed: 11922373]
27. Zhang Z, Li L, Yang W, et al. 2017 The effects of different doses of IGF-1 on cartilage and subchondral bone during the repair of full-thickness articular cartilage defects in rabbits. *Osteoarthritis Cartilage* 25: 309–320. [PubMed: 27662821]
28. Worster AA, Brower-Toland BD, Fortier LA, et al. Chondrocytic differentiation of mesenchymal stem cells sequentially exposed to transforming growth factor-beta1 in monolayer and insulin-like growth factor-I in a three-dimensional matrix. *J Orthop Res* 19: 738–749. [PubMed: 11518286]

29. Zhou Q, Li B, Zhao J, et al. 2016 IGF-I induces adipose derived mesenchymal cell chondrogenic differentiation in vitro and enhances chondrogenesis in vivo. *In Vitro Cell Dev Biol Anim.* 52: 356–364. [PubMed: 26822434]
30. Miller RE, Grodzinsky AJ, Cummings K, et al. Intraarticular injection of heparin-binding insulin-like growth factor 1 sustains delivery of insulin-like growth factor 1 to cartilage through binding to chondroitin sulfate. *Arthritis Rheum* 62:3686–3694. [PubMed: 20722014]
31. Tokunou T, Miller R, Patwari P, et al. 2008 Engineering insulin-like growth factor-1 for local delivery. *FASEB J* 22: 1886–1893. [PubMed: 18285400]
32. Wei X, Messner K. 1999 Maturation-dependent durability of spontaneous cartilage repair in rabbit knee joint. *J Biomed Mater Res* 46: 539–548. [PubMed: 10398015]

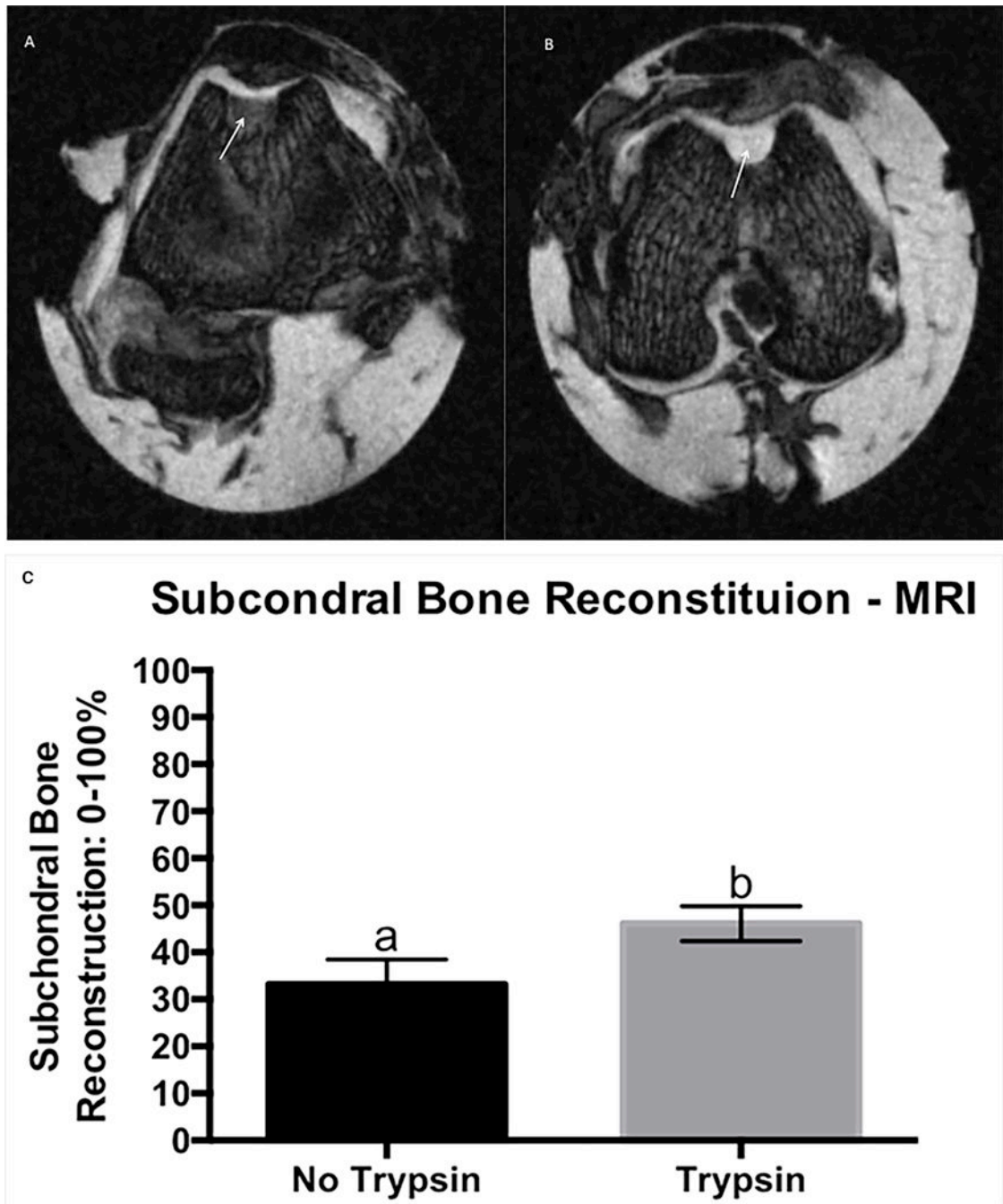


Figure 1. Transverse PDFS MRI image showing improved subchondral bone reconstitution (arrows) of the reparative tissue treated with trypsin (B), compared to its contralateral control (A), MRI score for main effect of trypsin on subchondral bone reconstitution, grading scale 0–100%, where 0% is no subchondral bone reconstitution and 100% is subchondral bone reconstituted to the level of surrounding tissue. Error bar represents standard error. Different letters mean statistical significant difference (C).

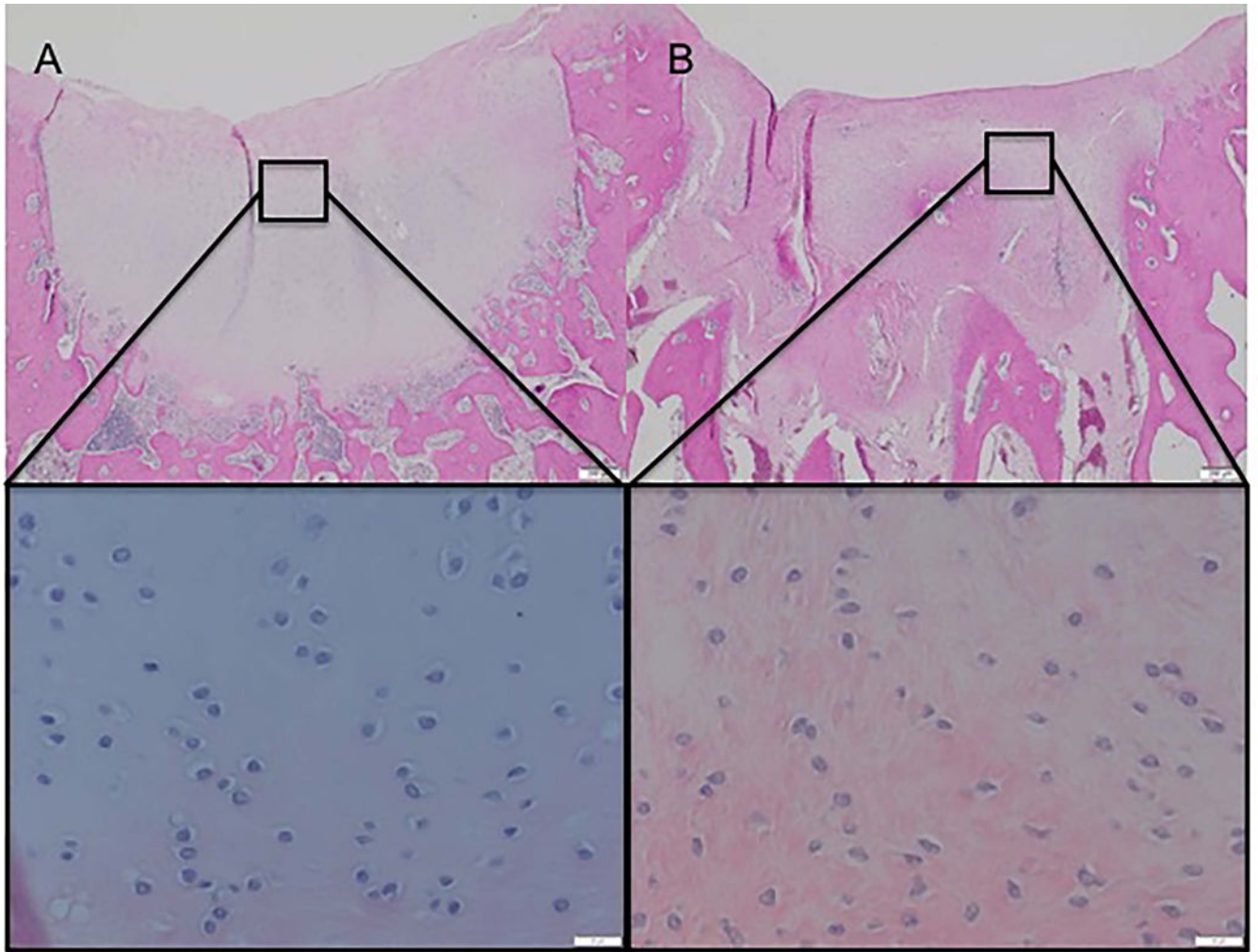


Figure 2. Improved cell morphology of a reparative tissue treated with trypsin (A) compared to its control not treated with trypsin (B). H&E staining, 10x and 40x magnification.

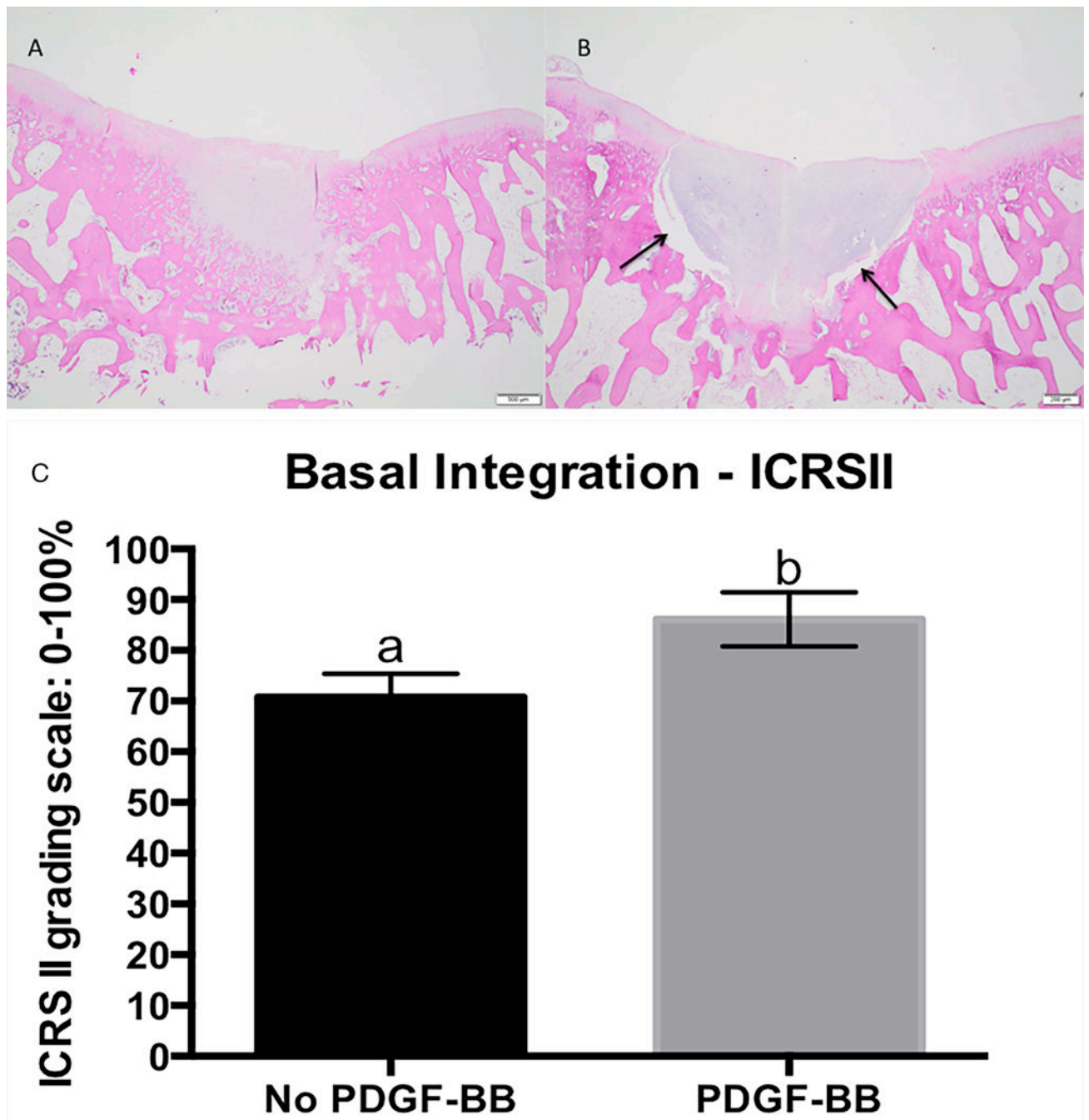


Figure 3. Improved basal integration on defect exposed to PDGF-BB (A) compared to its control not treat with PDGF-BB (B). Lack of basal integration is demonstrated by the space between subchondral bone and repairative tissue (arrows). H&E staining, 20 x magnification. Scale bar 500 μ m, histology score for main effect of PDGF-BB on basal integration. ICRSII grading scale: 0–100%, where 0 is completely abnormal and 100% is completely normal. Error bar represents standard error. Different letters mean statistical significant difference (C).

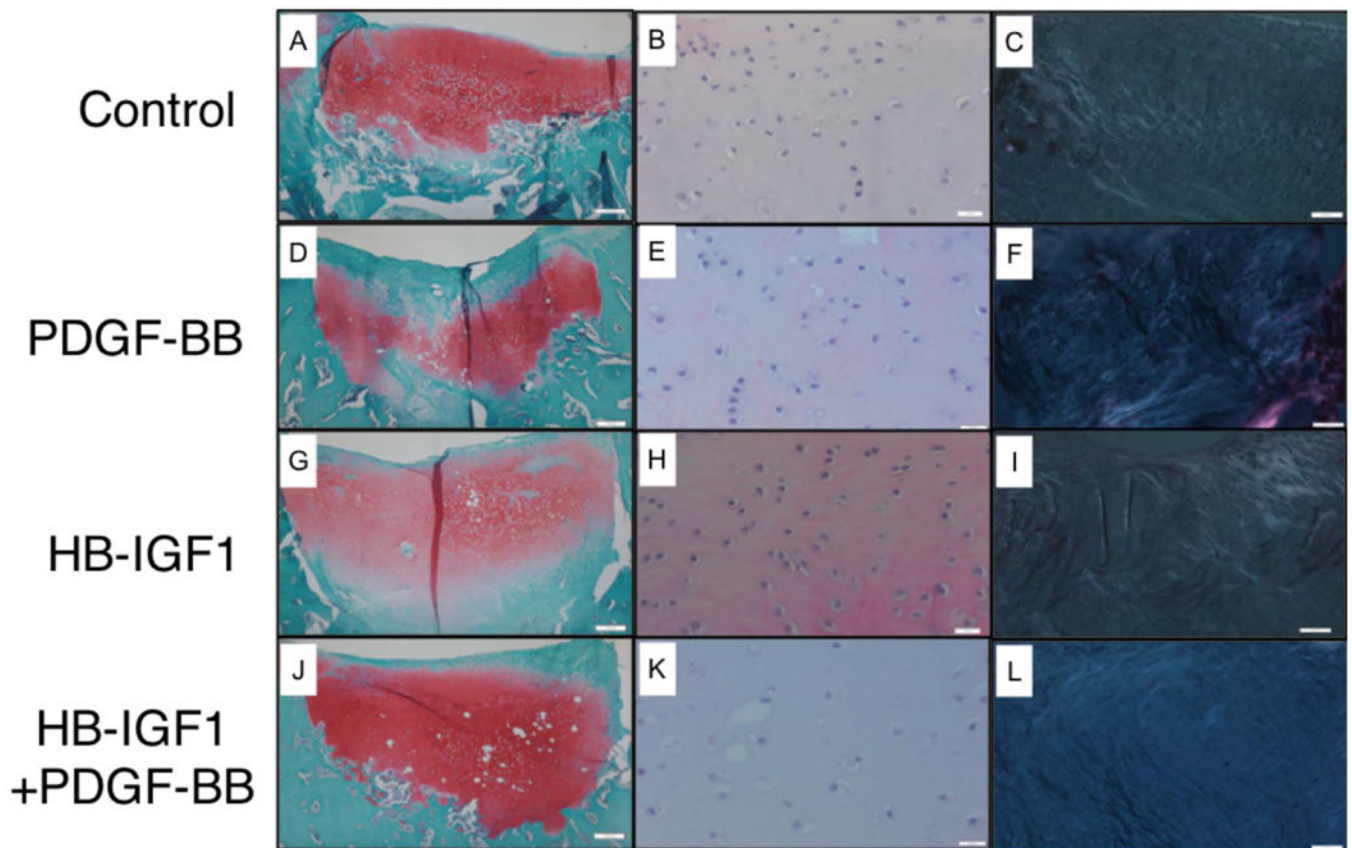


Figure 4. Representative histological images for main effect and interaction of HB-IGF1 and PDGF-BB on tissue morphology and chondrocyte morphology. Control (A, B, C), PDGF-BB (D, E, F), HB-IGF1 (G, H, I) and HB-IGF1 + PDGF-BB (J, K, L). Staining and magnification as follow: SOFG 10x (A, D, G, J), H&E 40x (B, E, H, K) and H&E under polarized microscopy 10x (C, F, I, L).

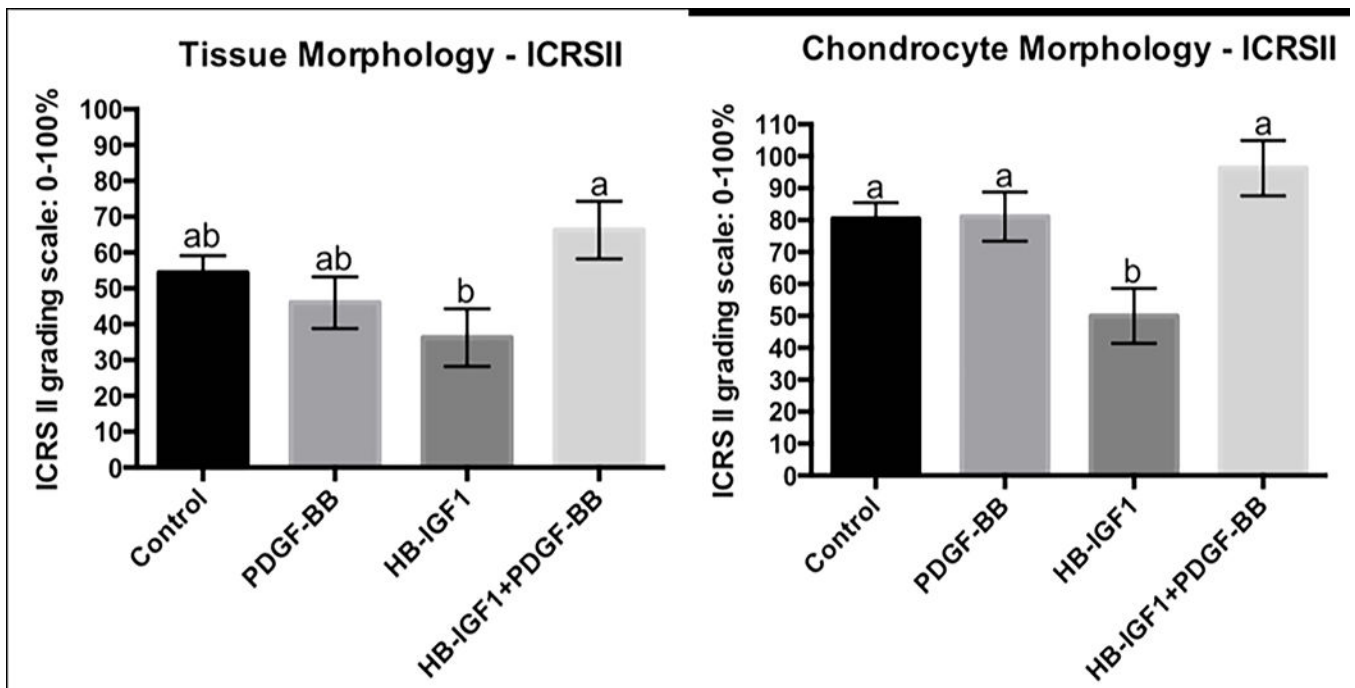


Figure 5. Histology score for main effect and interaction of HB-IGF1 and PDGF-BB on tissue and chondrocyte morphology. ICRSII grading scale: 0–100%, where 0 is completely abnormal and 100% is completely normal. Error bar represents standard error. Different letters mean statistical significant difference.

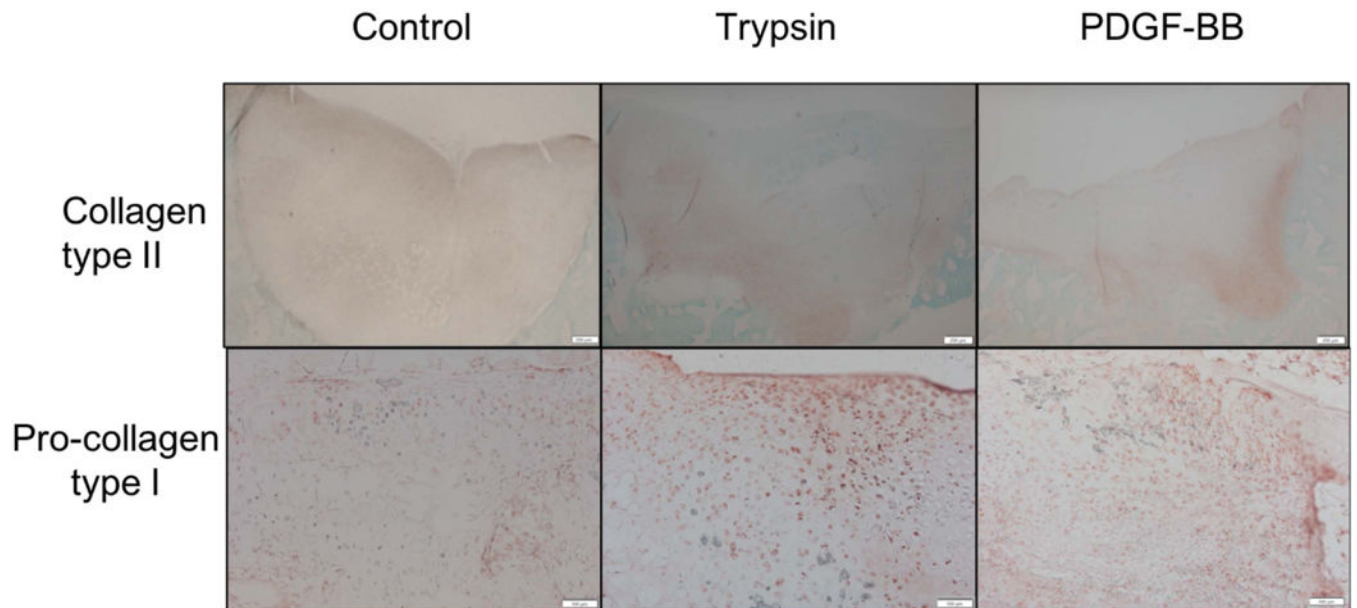


Figure 6. Representative images showing more pro-collagen type I (magnification 10x) immunohistostaining on defects treated with trypsin or PDGF-BB compared to control. Images of collagen type II (magnification 4x) immunohistochemistry are provided for reference.

Table 1:

Study design, treatment and control groups.

Treated limbs	Contra-lateral control limbs	Number of animals
KLD + Trypsin	KLD	8
KLD + HB-IGF1	KLD	8
KLD + Trypsin + HB-IGF1	KLD	8
KLD + Trypsin + PDGF-BB	KLD + Trypsin	8
KLD+ Trypsin + HB-IGF1+ PDGF-BB	KLD + Trypsin	8
KLD + Trypsin + PDGF-BB	Trypsin	4
KLD+ Trypsin + HB-IGF1+ PDGF-BB	Trypsin	4

Author Manuscript

Author Manuscript

Author Manuscript

Author Manuscript